JOURNAL OF MOLECULAR SPECTROSCOPY 94, 283–301 (1982)

Microwave Study of Vibration–Rotation Spectrum of Carbon Suboxide C_3O_2 in the 300- to 1000-GHz Frequency Range

E. N. KARYAKIN, A. F. KRUPNOV, AND S. M. SHAPIN

Institute of Applied Physics, Academy of Sciences of the USSR, Gorky, USSR

The submillimeter wave spectrum of the C_3O_2 molecule was investigated within the 300- to 1000-GHz range. The measured frequencies include 256 lines belonging to the ground vibrational state and to four excited vibrational states of ν_7. Rotational and centrifugal constants and constants of "ℓ" splitting for the ground and excited states ν_7^1, $2\nu_7^2$, $3\nu_7^3$, $4\nu_7^4$ as well as frequencies of purely vibrational transitions $\nu_7^1 \leftarrow 0$; $2\nu_7^2 \leftarrow \nu_7^1$; $3\nu_7^3 \leftarrow 2\nu_7^2$; $4\nu_7^4 \leftarrow 3\nu_7^3$ together with their correlation matrix were determined.

INTRODUCTION

Carbon suboxide C_3O_2 is a nonpolar molecule with anomalously low frequency and highly anharmonic bending vibration ν_7 whose frequency falls into the submillimeter wavelength range presently covered by microwave spectroscopic methods. For a more complete description of the structure of the C_3O_2 molecule and spectra it is highly advisable to study the bands corresponding to lower vibration–rotation transitions of the ν_7 vibration. In our previous paper (*1*) we described microwave investigation of the C_3O_2 spectrum in the 545- to 595-GHz range near the $\nu_7^1 \leftarrow 0$ band origin. Here, we treat the microwave C_3O_2 spectrum in the 300- to 1000-GHz range, where the origins of the vibration–rotation bands $\nu_7^1 \leftarrow 0$ and $2\nu_7^2 \leftarrow \nu_7^1$ are situated and quite a number of lines belonging to higher vibrational transitions of ν_7 have been observed. Spectral lines of the transitions $\nu_7^1 \leftarrow 0$; $2\nu_7^2 \leftarrow \nu_7^1$; $3\nu_7^3 \leftarrow 2\nu_7^2$; $4\nu_7^4 \leftarrow 3\nu_7^3$; $3\nu_7^1 \leftarrow 2\nu_7^0$ have been assigned in the experimental spectrum. A number of nonassigned lines also have been observed. Combined processing of the first four vibrational transitions has been carried out and corresponding rotational and centrifugal constants as well as frequencies of purely vibrational transitions have been obtained.

EXPERIMENTAL DETAILS

The carbon suboxide spectrum was investigated by a submillimeter microwave spectrometer RAD with a frequency-stabilized backward-wave oscillator (*2*) in the range 300 to 1000 GHz. Line frequencies were measured with a relative accuracy 10^{-7}–10^{-8} by a usual technique. Carbon suboxide was obtained by dehydration of malonic acid mixed with P_2O_5 and sand at the temperature 120–140°C, cleaned of carbon dioxide and acetic acid, and then stored at the liquid nitrogen temperature. The line frequency measurements were carried out at the room temperature of the absorption cell with C_3O_2 pressure of 0.3–1 Torr. At such a low pressure

0022-2852/82/080283-19$02.00/0

TABLE I

Experimental and Calculated Frequencies of the $\nu_7^1 \leftarrow 0$; $2\nu_7^2 \leftarrow \nu_7^1$; $3\nu_7^3 \leftarrow 2\nu_7^2$; $4\nu_7^4 \leftarrow 3\nu_7^3$ Transitions

Transition	Obs.Freq.in MHz (Est.Unc.)	Calc.Freq.in MHz (Est.Unc.)	O-C in KHz
	$\nu_7^1 \leftarrow 0$		
P(4)	527 080.573(70)	527 080.515(7)	58
P(6)	518 313.337(140)	518 313.251(7)	86
P(8)	509 677.435(61)	509 677.431(6)	4
P(10)	501 173.674(17)	501 173.652(6)	22
P(12)	492 802.664(70)	492 802.623(6)	41
P(14)	484 565.211(25)	484 565.160(6)	51
P(16)	476 462.241(41)	476 462.187(6)	55
P(18)	468 494.742(20)	468 494.724(6)	18
P(20)	460 663,892(17)	460 663.893(7)	- 1
P(22)	452 971.041(67)*	452 970.906(7)	135
P(24)	445 417.050(46)	445 417.059(7)	- 9
P(28)	430 732.385(34)	430 732.385(6)	0
P(30)	423 604.460(36)*	423 604.535(6)	- 75
P(32)	416 621.963(37)*	416 621.768(6)	195
P(40)	390 174.952(7)*	390 174.980(4)	- 29
P(42)	383 943.046(4)	383 943.045(3)	1
P(44)	377 866.581(10)	377 866.579(3)	2
P(48)	366 187.244(14)	366 187.260(2)	- 16
P(50)	360 587.997(4)	360 588.000(2)	- 3
P(52)	355 151.379(4)	355 151.374(2)	5
P(54)	349 879.125(5)	349 879.128(2)	- 3
P(58)	339 834.571(7)	339 834.570(3)	1
P(62)	330 467.435(13)	330 467.425(3)	10
P(64)	326 041.724(5)	326 041.722(3)	2
P(66)	321 789.810(6)*	321 789.838(4)	- 28
P(68)	317 713.101(8)	317 713.104(4)	- 3
P(70)	313 812.781(22)	313 812.760(4)	21
P(72)	310 089.998(13)*	310 089.950(4)	48
P(74)	306 545.714(5)	306 545.719(4)	- 5
P(76)	303 181.013(10)	303 181.005(4)	8
P(78)	299 996.636(11)	299 996.633(5)	3
P(80)	296 993.318(20)	296 993.312(6)	6
P(82)	294 171.636(15)	294 171.632(8)	4
P(84)	291 532.055(15)	291 532.058(13)	- 3
Q(2)	545 178.865(30)	545 178.856(7)	9
Q(6)	546 206.635(60)	546 206.702(6)	- 67
Q(8)	547 063.305(9)	547 063.294(5)	11
Q(10)	548 148.349(12)*	548 148.380(5)	- 31
Q(12)	549 461.997(10)	549 462.004(4)	- 7
Q(14)	551 004.203(21)	551 004.219(4)	- 16
Q(16)	552 775.100(13)	552 775.079(4)	21
Q(18)	554 774.623(7)	554 774.645(4)	- 22
Q(22)	559 460.129(14)	559 460.123(5)	6
Q(24)	562 146.153(48)	562 146.143(5)	10
Q(26)	565 061.047(28)	565 061.075(5)	- 28
Q(28)	568 204.947(50)	568 204.951(5)	- 4
Q(30)	571 577.759(43)	571 577.785(5)	- 26
Q(32)	575 179.581(22)	575 179.573(5)	8
Q(34)	579 010.292(17)	579 010.290(5)	2

TABLE I—*Continued*

Transiton	Obs.Freq.in MHz (Est.Unc.)	Calc.Freq.in MHz (Est.Unc.)	O-C in KHz
Q(36)	583 069.912(14)	583 069.881(4)	31
Q(38)	587 358.265(23)	587 358.262(4)	3
Q(40)	591 875.317(6)	591 875.315(4)	2
Q(42)	596 620.877(11)	596 620.881(4)	- 4
Q(44)	601 594.781(12)	601 594.759(4)	22
Q(46)	606 796.706(23)	606 796.700(4)	6
Q(48)	612 226.404(14)	612 226.403(5)	5
Q(50)	617 883.502(12)	617 883.515(5)	- 13
Q(52)	623 767.603(18)	623 767.618(6)	- 15
Q(54)	629 878.196(15)	629 878.234(7)	- 38
R(0)	549 571.046(200)	549 570.851(7)	195
R(2)	558 795.164(90)	558 795.117(7)	47
R(4)	568 149.650(247)	568 149,563(7)	87
R(6)	577 634.320(137)	577 634.229(8)	91
R(8)	587 249.241(65)	587 249.272(8)	- 31
R(10)	596 994.993(47)	596 994.963(8)	30
R(12)	606 871.727(43)	606 871.687(9)	40
R(14)	616 879.965(43)	616 879.938(9)	27
R(16)	627 020.280(46)	627 020.321(9)	- 41
R(52)	833 350.028(24)	833 350.052(10)	- 24
R(54)	846 222.179(15)	846 222.191(9)	- 12
R(56)	859 252.805(20)	859 252.809(8)	- 4
R(58)	872 443.393(25)	872 443.385(8)	8
R(60)	885 795.351(21)	885 795.358(8)	- 7
R(66)	926 833.251(9)	926 833.237(7)	14
R(70)	955 022.577(18)	955 022.580(10)	- 3
R(72)	969 369.803(23)	969 369.824(18)	- 21
	$2\nu_7^2 \leftarrow \nu_7^1$		
P(65)	632 064.853(33)	632 064.815(13)	38
P(67)	629 003.029(59)	629 003.056(13)	- 27
P(69)	626 087.479(29)	626 087.462(14)	17
P(71)	623 313.973(53)	623 313.969(14)	4
P(75)	618 176.329(35)	618 176.341(15)	- 12
P(77)	615 803.438(31)	615 803.424(16)	14
P(79)	613 555.061(40)	613 555.069(18)	- 8
P(83)	609 413.427(45)	609 413.441(24)	- 14
P(85)	607 510.838(85)	607 510.728(27)	110
P(89)	604 017.782(52)	604 017.771(32)	11
P(93)	600 910.126(68)	600 910.159(61)	- 33
P(50)	631 343.998(45)	631 343.982(8)	16
P(56)	612 639.204(20)	612 639.274(10)	- 70
P(58)	606 662.622(50)	606 662.592(10)	30
P(60)	600 817.430(50)	600 817.376(11)	54
P(62)	595 105.031(23)	595 105.021(12)	11
P(64)	589 526.874(80)	589 526.895(14)	- 21
P(66)	584 084.414(41)	584 084.346(16)	68
P(68)	578 778.675(46)	578 778.686(18)	- 11

TABLE I—*Continued*

Transition	Obs.Freq.in MHz (Est.Unc.)	Calc.Freq.in MHz (Est.Unc.)	O-C in KHz
Q(3)	828 279.830(58)*	828 280.222(9)	-392
Q(5)	828 729.344(50)	828 729.337(9)	7
Q(9)	830 225.997(31)	830 226:015(7)	- 18
Q(11)	831 273.325(31)	831 273.350(7)	- 25
Q(13)	832 519.806(27)	832 519.814(6)	- 8
Q(15)	833 965.193(16)	833 965.216(5)	- 23
Q(17)	835 609.373(27)	835 609.334(5)	39
Q(19)	837 451.933(31)	837 451.918(5)	15
Q(21)	839 492.687(20)	839 492.684(5)	3
Q(23)	841 731.348(8)*	841 731.319(5)	29
Q(25)	844 167.461(20)	844 167.477(5)	- 16
Q(27)	846 800.785(12)	846 800.783(5)	2
Q(29)	849 630.833(12)	849 630.828(5)	5
Q(31)	852 657.164(16)	852 657.174(5)	- 10
Q(33)	855 879.382(41)	855 879.348(5)	34
Q(35)	859 296.848(16)	859 296.850(5)	- 2
Q(37)	862 909.148(20)	862 909.142(5)	6
Q(39)	866 715.656(12)	866 715.659(5)	- 3
Q(41)	870 715.810(12)	870 715.801(5)	9
Q(43)	874 908.934(8)	874 908.937(5)	- 3
Q(45)	879 294.387(21)	879 294.401(5)	- 14
Q(47)	883 871.496(25)	883 871.498(6)	- 2
Q(55)	904 081.161(21)	904 081.121(9)	40
Q(57)	909 604.791(21)	909 604.778(10)	13
Q(59)	915 315.190(30)	915 315.195(11)	- 5
Q(61)	921 211 177(18)*	921 211.446(12)	-269
Q(71)	953 445.398(18)	953 445.416(13)	- 18
Q(73)	960 435.329(14)	960 435.327(10)	2
Q(75)	967 603.649(18)	967 603.645(17)	4
Q(2)	828 057.403(115)*	828 056.959(9)	444
Q(4)	828 234.802(93)	828 234.721(9)	81
Q(6)	828 514.140(50)	828 514.125(8)	15
Q(8)	828 895.261(31)	828 895.251(8)	10
Q(12)	829 963.117(27)	829 963.134(6)	- 17
Q(14)	830 650.474(27)	830 650.179(6)	295
Q(16)	831 439.514(24)	831 439.518(5)	- 4
Q(18)	832 331.324(20)	832 331.324(4)	- 15
Q(20)	833 325.827(16)	833 325.837(4)	- 10
Q(22)	834 423.207(16)	834 423.211(4)	- 4
Q(24)	835 623.628(20)	835 623.657(4)	- 29
Q(26)	836 927.378(16)	836 927.365(4)	13
Q(28)	838 334.500(16)	838 334.505(4)	- 5
Q(30)	839 845.235(8)	839 845.228(4)	7
Q(32)	841 459.648(8)	841 459.652(4)	- 4
Q(34)	843 177.854(15)	843 177.857(4)	- 3
Q(36)	844 999.876(12)	844 999.878(4)	- 2
Q(38)	846 925.695(20)	846 925.693(4)	2
Q(40)	848 955.210(12)	848 955.220(4)	- 10
Q(42)	851 088.297(12)	851 088.301(4)	- 4
Q(44)	853 324.704(16)	853 324.702(4)	2

TABLE I—*Continued*

Transition	Obs.Freq.in MHz (Est.Unc.)	Calc.Freq.in MHz (Est.Unc.)	O-C in KHz
Q(46)	855 664.114(20)	855 664.098(5)	16
Q(48)	858 106.086(16)	858 106.069(5)	17
Q(50)	860 650.091(20)	860 650.088(5)	3
Q(52)	863 295.519(12)	863 295.520(4)	- 1
Q(54)	866 041.597(8)	866 041.607(4)	- 10
Q(56)	868 887.466(20)	868 887.470(4)	- 4
Q(58)	871 832.107(8)	871 832.098(5)	9
Q(60)	874 874.347(21)	874 874.343(5)	4
Q(62)	878 012.904(25)	878 012.921(6)	- 17
Q(64)	881 246.388(29)	881 246.405(8)	- 17
Q(66)	884 573.223(17)	884 573.227(9)	- 4
Q(68)	887 991.690(37)	887 991.678(10)	12
Q(78)	906 388.996(21)	906 389.025(17)	- 29
Q(82)	914 315.035(47)	914 314.982(20)	53
Q(84)	918 389.624(73)	918 389.596(22)	28
Q(86)	922 535.170(52)	922 535.163(29)	7
Q(88)	926 749.065(60)	926 749.064(47)	1
R(1)	837 257.081(132)	837 257.075(9)	6
R(3)	846 732.667(63)	846 732.771(8)	-104
R(5)	856 407.556(37)	856 407.576(8)	- 20
R(7)	866 281.092(28)	866 281.115(8)	- 23
R(11)	886 622.511(25)	886 622.515(7)	- 4
R(15)	907 752.402(30)	907 752.411(6)	- 9
R(17)	918 611.283(34)	918 611.260(6)	23
R(23)	952 352.754(18)	952 352.740(7)	14
R(25)	963 984.709(18)	963 984.705(7)	4
R(2)	841 896.533(47)	841 896.484(9)	49
R(4)	851 300.416(28)	851 300.334(8)	82
R(6)	860 805.664(28)*	860 805.494(8)	170
R(8)	870 411.979(50)	870 411.992(8)	- 13
R(10)	880 119.945(46)	880 119.933(7)	12
R(12)	889 929.492(50)	889 929.496(7)	- 4
R(18)	919 970.827(22)	919 970.816(6)	12
R(24)	950 940.136(36)	950 940.125(5)	11
R(28)	972 109.634(5)	972 109.632(5)	2
	$3\nu_7^3 \leftarrow 2\nu_7^2$		
P(11)	974 076.286(32)	974 076.295(16)	- 9
P(13)	965 631.862(63)	965 631.824(13)	38
P(15)	957 323.771(27)	957 323.761(11)	10
P(23)	925 457.001(26)	925 457.003(12)	- 2
P(25)	917 831.849(43)	917 831.874(12)	- 25
P(29)	902 991.450(21)	902 991.446(12)	4
P(35)	881 754.330(21)	881 754.343(10)	- 13
P(39)	868 277.155(12)	868 277.149(9)	6
P(41)	861 742.226(28)	861 742.238(8)	- 12
P(43)	855 342.784(16)	855 342.780(9)	4
P(45)	849 078.470(32)	849 078.472(11)	- 2

TABLE I—*Continued*

Transition	Obs.Freq.in MHz (Est.Unc.)	Calc.Freq.in MHz (Est.Unc.)	O-C in MHz
P(47)	842 948.964(20)	842 948.973(12)	- 9
P(49)	836 953.894(24)	836 953.895(13)	- 1
P(51)	831 092.816(24)	831 092.811(22)	5
P(12)	969 839.867(23)	969 839.878(15)	- 11
P(16)	953 229.735(27)	953 229.724(11)	11
P(24)	921 671.256(56)	921 671.229(13)	28
P(26)	914 130.959(34)	914 130.960(13)	- 1
P(28)	906 731.672(26)	906 731.675(12)	- 3
P(32)	892 358.912(42)	892 358.874(10)	38
P(34)	885 386.883(25)	885 386.882(9)	1
P(36)	878 558.899(17)	878 558.919(9)	- 20
P(38)	871 875.865(21)	871 875.863(9)	2
P(40)	865 338.646(16)	865 338.636(8)	10
P(42)	858 948.218(28)	858 948.206(8)	12
P(44)	852 705,583(16)	852 705.589(9)	- 6
P(46)	846 611.837(24)	846 611.843(10)	- 6
P(48)	840 668.073(16)	840 668.067(11)	6
P(50)	834 875.395(27)	834 875.402(10)	- 7
P(52)	829 235.021(16)	829 235.021(15)	0
	$4\nu_7^4 \leftarrow 3\nu_7^3$		
P(47)	991 106.330(50)	991 106.311(42)	19
P(49)	984 856.972(50)	984 856.982(23)	- 10
P(53)	972 752.795(14)	972 752.808(12)	- 13
P(55)	966 898.634(50)	966 898.653(9)	- 20
P(57)	961 176.961(9)	961 176.947(6)	14
P(59)	955 588.075(9)	955 588.084(7)	- 9
P(71)	924 869.827(30)	924 869.844(23)	- 17
P(73)	920 224.148(43)	920 224.107(19)	41
P(75)	915 715.367(26)	915 715.361(19)	6
P(79)	907 111.542(26)	907 111.556(23)	- 14
P(81)	903 017.975(47)	903 017.954(44)	21
P(50)	981 743.585(50)	981 743.562(24)	23
P(54)	969 748.370(23)	969 748.370(14)	0
P(56)	963 945.189(18)	963 945.192(11)	- 3
P(58)	958 271.554(23)	958 271.555(12)	- 1
P(60)	952 727.367(27)	952 727.365(15)	2
P(70)	926 941.984(18)	926 941.984(17)	0
P(72)	922 170.158(52)	922 170.154(21)	4
P(78)	908 617.926(38)	908 617.927(38)	- 1

the spectrum (and, hence, the composition of the substance in the cell) was stable for several hours. When measuring the line frequencies given in Table I, the C_3O_2 pressure was at 0.4 Torr. The absorption cell was made of stainless steel with Teflon windows to transmit radiation and contained an acoustic receiver-microphone constructed of stainless steel, glass, and Teflon.[1]

Figure 1 shows a part of a record of the C_3O_2 spectrum in the range 828 to 860 GHz containing lines of the *R* branch of the transition $\nu_7^1 \leftarrow 0$, the *Q* branch (with even and odd *J*) and the *R* branch (with even and odd *J*) of the transition $2\nu_7^2 \leftarrow \nu_7^1$, and the *P* branch (with even and odd *J*) of the transition $3\nu_7^3 \leftarrow 2\nu_7^2$. The

[1] It is to be noted, that in several months of investigation of the C_3O_2 spectrum the Teflon element of the microphone turned pink violet to a depth of 0.5 mm, the surface layer was just slightly colored.

measured line frequencies are listed in Table I. Figure 1 also displays a sequence of lines (marked by * (asterisk)) which we assign to the transition $3\nu_7^1 \leftarrow 2\nu_7^0$. The measured frequencies of these lines are presented in Table II. Figure 2 shows a part of a record of the C_3O_2 spectrum in the range 965 to 990 GHz containing lines of the R branch of the transition $\nu_7^1 \leftarrow 0$, the Q branch (with odd J) and the R branch (with even and odd J) of the transition $2\nu_7^2 \leftarrow \nu_7^1$, the P branch (with even and odd J) of the transition $3\nu_7^3 \leftarrow 2\nu_7^2$, the P branch (with even and odd J) of the transition $4\nu_7^4 \leftarrow 3\nu_7^3$ and, finally, the P branch of the transition $3\nu_7^1 \leftarrow 2\nu_7^0$, which corresponds to the lines mentioned above (see Fig. 1) marked by an asterisk. Figure 2 also shows two line sequences marked by crosses (+) and arrows (↓). We assigned the spectral lines marked by crosses to the transition $4\nu_7^2 \leftarrow 3\nu_7^1$; their measured frequencies are listed in Table III. At present the spectral lines marked by arrows whose measured frequencies are given in Table IV, are not assigned to any known transition. Besides these lines records showed a considerable number of weak lines which we did not assign. We observed also the known lines of water which were present in the sample as an impurity.

SPECTRUM PROCESSING

The following expressions for energies of vibration–rotation spectra of the C_3O_2 molecule were used in the processing of the results of the experiment.

(a) The ground vibrational state

$$E_{v,r} = E_v + E_r = E_v + BJ(J+1) - DJ^2(J+1)^2 + HJ^3(J+1)^3 + LJ^4(J+1)^4 + NJ^5(J+1)^5;$$

(b) the excited vibrational state ν_7^1

$$\begin{aligned} E_{v,r} = E_v + E_r = E_v &+ B[J(J+1)-1] + (-1)^J(q_0/2)J(J+1) \\ &- D[J(J+1)-1]^2 + (-1)^J(q_1/2)J(J+1)[J(J+1)-1] \\ &+ H[J(J+1)-1]^3 + (-1)^J(q_2/2)J(J+1)[J(J+1)-1]^2 \\ &+ L[J(J+1)-1]^4 + (-1)^J(q_3/2)J(J+1)[J(J+1)-1]^3 + N[J(J+1)-1]^5; \end{aligned}$$

(c) the excited vibrational state $2\nu_7^2$

$$\begin{aligned} E_{v,r} = E_v + E_r = E_v &+ B[J(J+1)-4] \\ &+ (-1)^{(J+1)}(q_0/2)J(J+1)[J(J+1)-2] - D[J(J+1)-4]^2 \\ &+ (-1)^{(J+1)}(q_1/2)J(J+1)[J(J+1)-2][J(J+1)-4] + H[J(J+1)-4]^3 \\ &+ (-1)^{(J+1)}(q_2/2)J(J+1)[J(J+1)-2][J(J+1)-4]^2 + L[J(J+1)-4]^4 \\ &+ (-1)^{(J+1)}(q_3/2)J(J+1)[J(J+1)-2][J(J+1)-4]^3 + N[J(J+1)-4]^5; \end{aligned}$$

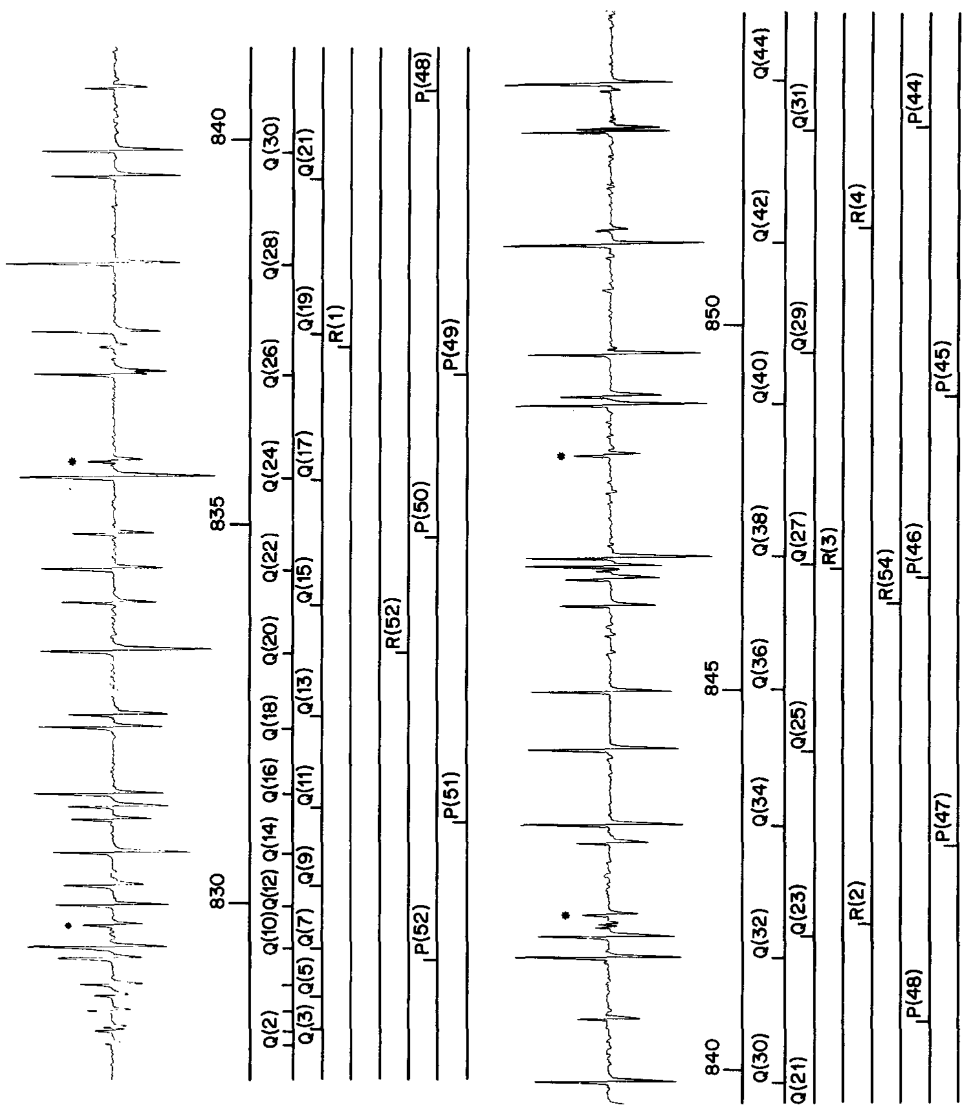

830
835
840
845
850
Q(2) Q(3) Q(5) Q(7) Q(9) Q(10) Q(11) Q(12) Q(13) Q(14) Q(15) Q(16) Q(17) Q(18) Q(19) Q(20) Q(21) Q(22) Q(24) Q(26) Q(28) Q(30)
R(1) R(52)
P(48) P(49) P(50) P(51) P(52)
Q(21) Q(23) Q(25) Q(27) Q(29) Q(30) Q(31) Q(32) Q(34) Q(36) Q(38) Q(40) Q(42) Q(44)
R(2) R(3) R(4) R(54)
P(44) P(45) P(46) P(47) P(48)

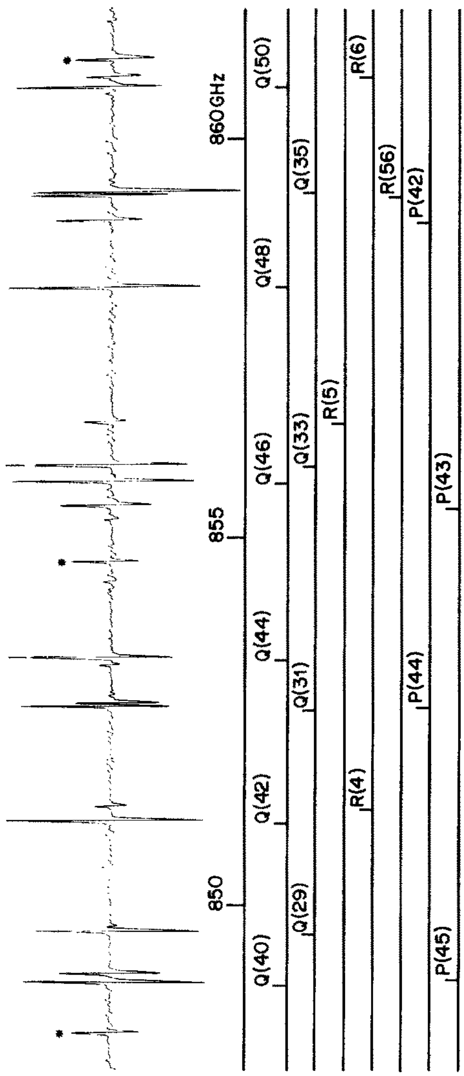

FIG. 1. Vibration–rotation spectrum of C_3O_2 around 845 GHz.

TABLE II

Experimental Frequencies of the $3\nu_7^1 \leftarrow 2\nu_7^0$ Transition

Transition	Obs.Freq.in MHz (Est.Unc.)
P(24)	989 754.50(10)
P(26)	981 845.40(10)
P(28)	974 032.702(14)
P(30)	966 315.193(14)
P(32)	958 691.840(9)
P(34)	951 161.324(36)
P(42)	921 940.218(22)
P(44)	914 852.677(30)
P(46)	907 648.949(38)
P(52)	887 323.316(37)
P(54)	880 637.179(50)
P(56)	874 025.769(21)
P(58)	867 487.198(16)
P(60)	861 019.453(16)
P(62)	854 620.629(28)
P(64)	848 288.725(32)
P(66)	842 021.937(30)

(d) the excited vibrational state $3\nu_7^3$

$$E_{v,r} = E_v + E_r = E_v + B[J(J+1) - 9] + (-1)^J (q_0/2)[J(J+1) - 2] \times [J(J+1) - 6] - D[J(J+1) - 9]^2 + (-1)^J (q_1/2)[J(J+1) - 2] \times [J(J+1) - 6][J(J+1) - 9] - H[J(J+1) - 9]^3 + (-1)^J (q_2/2) \times [J(J+1) - 2][J(J+1) - 6][J(J+1) - 9]^2 + L[J(J+1) - 9]^4 + (-1)^J (q_3/2)[J(J+1) - 2][J(J+1) - 6][J(J+1) - 9]^3 + N[J(J+1) - 9]^5;$$

(e) the excited vibrational state $4\nu_7^4$

$$E_{v,r} = E_v + E_r = E_v + B[J(J+1) - 16] + (-1)^{(J+1)} (q_0/2) \times [J(J+1) - 6][J(J+1) - 12] - D[J(J+1) - 16]^2 + (-1)^{(J+1)} (q_1/2)[J(J+1) - 6][J(J+1) - 12][J(J+1) - 16] + H[J(J+1) - 16]^3 + (-1)^{(J+1)} (q_2/2)[J(J+1) - 6][J(J+1) - 12] \times [J(J+1) - 16]^2 + L[J(J+1) - 16]^4 + (-1)^{(J+1)} (q_3/2)[J(J+1) - 6] \times [J(J+1) - 12][J(J+1) - 16]^3 + N[J(J+1) - 16]^5;$$

where $E_{v,r}$ is the vibration–rotation energy, E_v is the vibrational energy, E_r is the rotational energy, B, D, H, L, N are the rotational and centrifugal constants of the

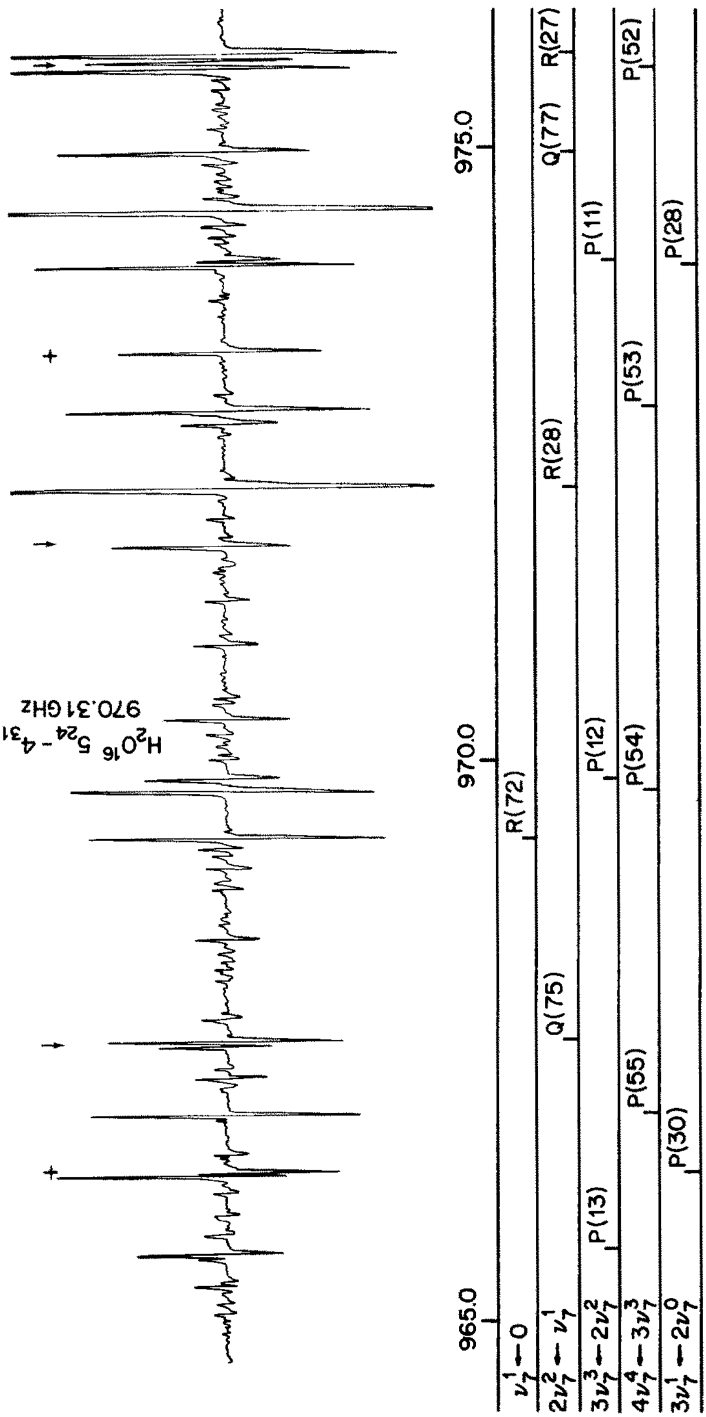

FIG. 2. Vibration–rotation spectrum of C_3O_2 around 980 GHz.

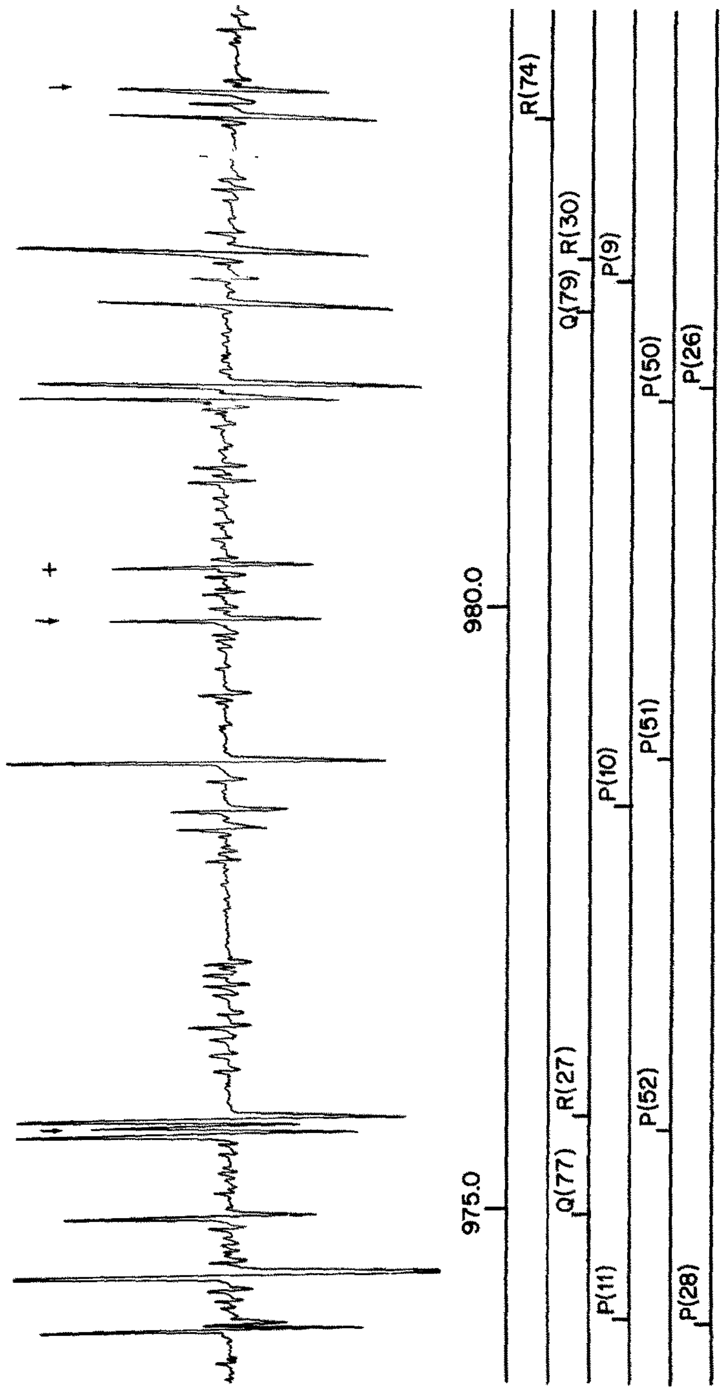

FIG. 2.—*Continued*

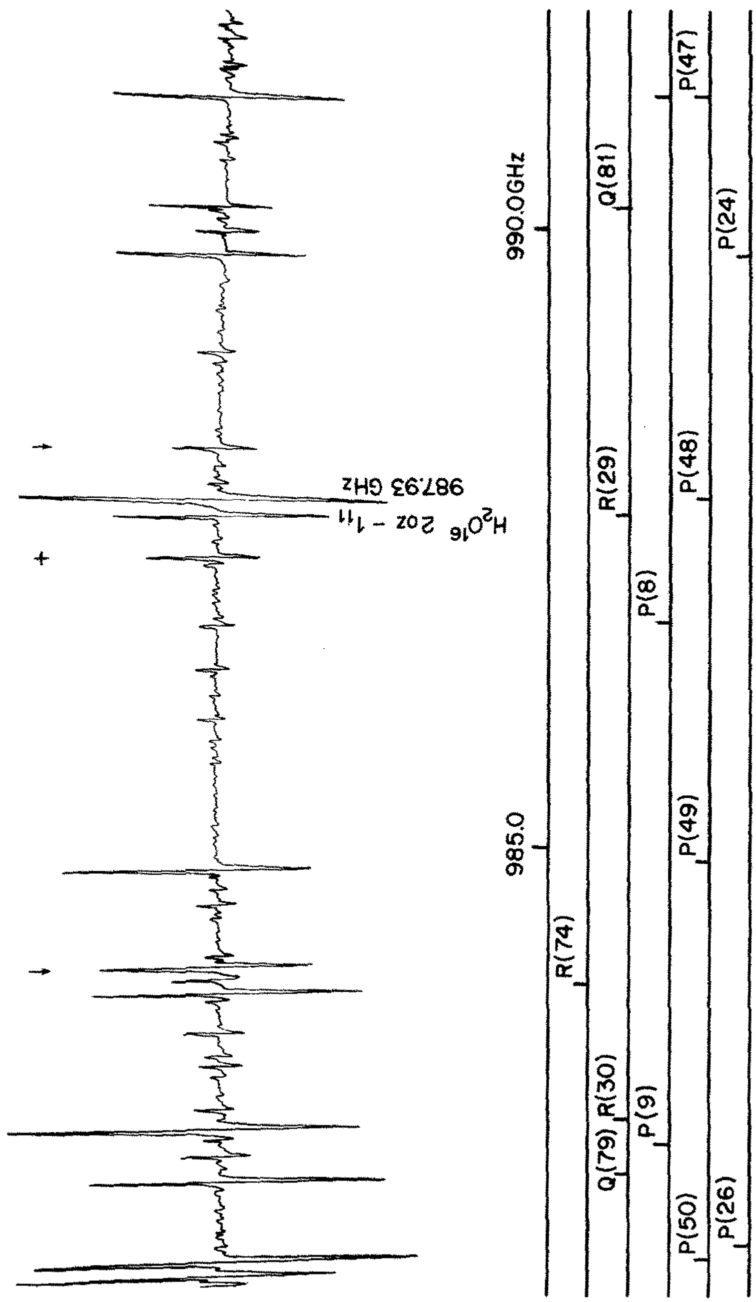

FIG. 2.—*Continued*

TABLE III

Experimental Frequencies of the $4\nu_7^2 \leftarrow 3\nu_7^1$ Transition

Obs.Freq.in MHz (Est.Unc)
987 496.646(50)
980 361.447(50)
973 312.184(14)
966 348.989(9)
959 472.222(14)
952 682.099(40)
926 393.834(48)
920 041.610(100)
913 777.981(39)
907 603.944(55)

corresponding vibrational state, and q_0, q_1, q_2, q_3 are the corresponding constants of "ℓ"-splitting.

Preliminary description was carried out by the least-squares method using a polynomial in powers of J for each branch of the transitions $\nu_7^1 \leftarrow 0$; $2\nu_7^2 \leftarrow \nu_7^1$; $3\nu_7^3 \leftarrow 2\nu_7^2$. A few spectral lines whose values of the calculated frequencies differ from the experimental ones by values much higher than the experimental errors (marked in Table I by an asterisk) were excluded from further processing.

Diagrams of energy levels for C_3O_2 transitions (see, for example, (*4*)) show that a set of available experimental data in the present investigation allows a complete description of rotational levels in the ground and excited vibrational states ν_7^1; $2\nu_7^2$; $3\nu_7^3$; $4\nu_7^4$. Therefore, further processing included all the observed lines (i.e.,

TABLE IV

Experimental Frequencies of the Unknown Transition

Obs.Freq.in MHz (Est.Unc.)
988 318.654(50)
984 086.720(50)
971 635.596(19)
967 546.237(14)
963 478.127(63)
959 426.515(18)
955 386.935(40)
951 355.640(89)

TABLE V

Spectroscopic Constants of the C_3O_2 Molecule in the Ground and Excited Vibrational States ν_7^1; $2\nu_7^2$; $3\nu_7^3$; $4\nu_7^4$ and Their Correlation Matrix

$0000\,0^0 0^0 0^0$	B	2 265.358915	(302)	MHz	1		
	D	1 162.495	(265)	Hz	0.943	1	
	H	0.0221488	(933)	Hz	0.872	0.980	1
	L	-0.4307	(148)x10^{-6}	Hz	-0.796	-0.933	-0.985
	N	0.9012	(889)x10^{-11}	Hz	0.715	0.868	0.944
$0000\,0^0 0^0 1^1$	ν_0	547 295.3332	(69)	MHz	0.230	0.260	0.278
	B	2 287.777323	(303)	MHz	0.9963	0.935	0.859
	q_0	6.1294155	(79)	MHz	-0.312	-0.399	-0.461
	D	995.877	(271)	Hz	0.942	0.9957	0.972
	q_1	-138.4959	(87)	Hz	0.474	0.598	0.667
	H	0.0125966	(980)	Hz	0.873	0.979	0.995
	q_2	0.0025335	(29)	Hz	-0.514	-0.657	-0.739
	L	-0.2285	(161)x10^{-6}	Hz	-0.798	-0.935	-0.983
	q_3	-0.2406	(30)x10^{-7}	Hz	0.509	0.660	0.755
	N	0.739	(100)x10^{-11}	Hz	0.716	0.870	0.944
$0000\,0^0 0^0 2^2$	ν_0	834 919.4061	(91)	MHz	-0.211	-0.212	-0.203
	B	2 306.596033	(308)	MHz	0.9927	0.937	0.864
	q_0	59.0505	(63)	Hz	-0.130	-0.068	-0.023
	D	995.408	(278)	Hz	0.934	0.9913	0.969
	q_1	0.0044379	(53)	Hz	0.022	-0.054	-0.097
	H	0.005276	(101)	Hz	0.865	0.973	0.989
	q_2	-0.1237	(13)x10^{-6}	Hz	0.046	0.130	0.175
	L	-0.610	(165)x10^{-7}	Hz	-0.794	-0.929	-0.977
	q_3	-0.233	(13)x10^{-11}	Hz	-0.087	-0.177	-0.225
	N	0.908	(103)x10^{-11}	Hz	0.716	0.866	0.938
$0000\,0^0 0^0 3^3$	ν_0	1 034 639.296	(27)	MHz	0.287	0.283	0.267
	B	2 323.52361	(33)	MHz	0.903	0.839	0.766
	q_0	0.0561	(24)	Hz	-0.031	-0.023	-0.016
	D	968.01	(34)	Hz	0.770	0.803	0.776
	q_1	0.001002	(247)	Hz	0.004	-0.003	-0.006
	H	0.00541	(14)	Hz	0.593	0.650	0.648
	q_2	0.6378	(616)	Hz	0.005	0.010	0.012
	L	-0.102	(22)	Hz	-0.432	-0.486	-0.496
$0000\,0^0 0^0 4^4$	ν_0	1 191 642.9	(14)	MHz	0.025	0.028	0.028
	B	2 339.2146	(15)	MHz	0.168	0.148	0.131
	D	960.27	(64)	Hz	0.380	0.391	0.374
	q_1	-0.15	(10)x10^{-4}	Hz	-0.043	-0.048	-0.045
	H	0.00498	(17)	Hz	0.500	0.545	0.541
	q_2	0.177	(38)x10^{-7}	Hz	0.044	0.045	0.041
	L	-0.104	(24)x10^{-6}	Hz	-0.419	-0.471	-0.479
	q_3	0.150	(25)x10^{-11}	Hz	-0.039	-0.030	-0.022

TABLE V—*Continued*

1						
-0.987	1					
-0.291	0.296	1				
-0.780	0.697	0.162	1			
0.512	-0.549	-0.190	-0.308	1		
-0.921	0.853	0.197	0.941	-0.402	1	
-0.718	0.750	0.252	0.464	-0.940	0.594	1
-0.976	0.932	0.219	0.868	-0.471	0.980	0.670
0.801	-0.842	-0.273	-0.499	0.859	-0.647	-0.977
0.9954	-0.979	-0.238	-0.789	0.529	-0.931	-0.729
-0.829	0.882	0.279	0.492	-0.789	0.647	0.935
-0.985	0.9960	0.252	0.704	-0.571	0.862	0.767
0.188	-0.169	-0.024	-0.210	-0.090	-0.211	0.019
-0.785	0.701	0.160	0.9961	-0.284	0.943	0.446
-0.014	0.044	0.002	-0.128	-0.295	-0.064	0.206
-0.919	0.850	0.193	0.933	-0.368	0.9952	0.566
0.130	-0.155	-0.042	0.023	0.333	-0.056	-0.295
-0.970	0.925	0.214	0.860	-0.431	0.973	0.635
-0.208	0.232	0.069	0.043	-0.347	0.130	0.345
0.987	-0.969	-0.231	-0.785	0.485	-0.925	-0.689
0.261	-0.288	-0,088	-0.082	0.353	-0.174	-0.375
-0.976	0.985	0.244	0.705	-0.526	0.859	0.725
-0.249	0.228	0.053	0.287	-0.097	0.283	0.149
-0.690	0.611	0.139	0.907	-0.243	0.845	0.384
0.010	-0.005	-0.003	-0.031	-0.043	-0.022	0.025
-0.727	0.665	0.149	0.770	-0.281	0.808	0.438
0.009	-0.011	-0.004	0.004	0.031	-0.003	-0.028
-0.623	0.583	0.131	0.591	-0.262	0.652	0.393
-0.013	0.014	0.005	0.005	-0.019	0.010	0.022
0.486	-0.464	-0.106	-0.429	0.221	-0.487	-0.320
-0.027	0.0260	0.006	0.026	-0.018	0.028	0.021
-0.113	0.099	0.023	0.169	-0.029	0.150	0.056
-0.347	0.315	0.071	0.380	-0.123	0.393	0.201
0.041	-0.038	-0.015	0.042	0.009	-0.047	-0.031
-0.519	0.485	0.110	0.498	-0.211	0.546	0.322
-0.036	0.032	0.014	0.043	0.007	0.044	0.017
0.470	-0.448	-0.103	-0.416	0.210	-0.471	-0.307
0.016	-0.010	-0.005	-0.038	-0.044	-0.029	0.022

TABLE V—*Continued*

1						
-0.736	1					
-0.984	0.805	1				
0.747	-0.988	-0.829	1			
0.940	-0.853	-0.985	0.888	1		
-0.201	0.023	0.185	-0.045	-0.166	1	
0.872	-0.487	-0.793	0.484	0.708	-0.284	1
-0.017	-0.163	-0.022	0.143	0.053	0.208	-0.159
0.976	-0.625	-0.928	0.629	0.859	-0.278	0.943
-0.102	0.267	0.137	-0.248	-0.163	-0.187	0.055
0.9933	-0.705	-0.976	0.720	0.932	-0.265	0.872
0.178	-0.331	-0.214	0.318	0.240	0.164	0.012
-0.977	0.770	0.9909	-0.797	-0.974	0.246	-0.798
-0.226	0.374	0.265	-0.368	-0.294	-0.143	-0.053
0.935	-0.815	-0.977	0.854	0.988	-0.222	0.717
0.269	-0.164	-0.251	0.165	0.230	-0.084	0.289
0.773	-0.419	-0.697	0.413	0.617	-0.256	0.910
-0.015	-0.016	0.008	0.012	-0.003	0.036	-0.036
0.782	-0.481	-0.735	0.481	0.672	-0.226	0.777
-0.007	0.024	0.010	-0.021	-0.012	-0.020	0.008
0.652	-0.434	-0.629	0.439	0.589	-0.178	0.598
0.012	-0.021	-0.013	0.020	0.014	0.010	0.003
-0.498	0.355	0.490	-0.362	-0.468	0.130	-0.435
0.029	-0.022	-0.028	0.021	0.026	-0.004	0.025
0.132	-0.062	-0.116	0.061	0.099	-0.052	0.170
0.377	-0.223	-0.351	0.223	0.319	-0.116	0.384
-0.044	0.037	0.041	-0.036	-0.038	0.009	-0.042
0.545	-0.357	-0.524	0.361	0.489	-0.154	0.505
0.040	-0.025	-0.036	0.026	0.032	-0.018	0.044
-0.481	0.341	0.473	-0.348	-0.452	0.128	-0.422
-0.021	-0.013	0.014	0.009	-0.008	0.040	-0.043

TABLE V—*Continued*

1										
-0.112	1									
-0.962	-0.004	1								
-0.087	0.981	-0.024	1							
0.896	0.078	-0.982	0.098	1						
0.070	-0.934	0.033	-0.985	-0.105	1					
-0.833	-0.124	0.947	-0.147	-0.9903	0.156	1				
-0.057	0.867	-0.037	0.942	0.107	-0.986	-0.160	1			
-0.048	0.284	0.016	0.270	0.005	-0.253	-0.018	0.233	1		
-0.145	0.844	0.052	0.774	0.007	-0.701	-0.043	0.624	-0.088	1	
0.165	-0.030	-0.154	-0.026	0.140	0.023	-0.128	-0.020	0.069	-0.090	1
-0.089	0.810	-0.005	0.785	0.064	-0.739	-0.099	0.678	-0.211	0.934	-0.128
-0.097	0.002	0.103	0.001	-0.102	-0.001	0.099	0.001	-0.094	0.075	-0.983
-0.053	0.655	-0.021	0.655	0.069	-0.633	-0.098	0.594	-0.341	0.824	-0.175
0.050	0.007	-0.062	0.007	0.066	-0.006	-0.067	0.005	0.110	-0.073	0.951
0.028	-0.490	0.025	-0.500	-0.061	0.493	0.084	-0.472	0.423	-0.705	0.216
0.020	0.027	-0.022	0.027	0.022	-0.026	-0.021	0.024	-0.006	0.028	0.121
-0.058	0.150	0.040	0.134	-0.027	-0.119	0.019	0.104	-0.006	0.183	-0.169
-0.076	0.396	0.028	0.380	0.003	-0.355	-0.022	0.324	-0.090	0.455	-0.222
0.025	-0.045	0.010	-0.041	-0.031	0.036	0.043	-0.031	-0.126	0.040	-0.864
-0.067	0.550	0.004	0.549	0.039	-0.529	-0.065	0.496	-0.276	0.690	-0.261
-0.075	0.045	0.041	0.041	-0.017	-0.036	0.002	0.031	0.137	-0.045	0.782
0.037	-0.475	0.015	-0.485	-0.050	0.477	0.073	-0.457	0.410	-0.684	0.263
0.177	-0.037	-0.162	-0.032	0.145	0.029	-0.130	-0,026	0.057	-0.090	0.946

TABLE V—*Continued*

1								
0.124	1							
0.962	0.185	1						
-0.130	-0.991	-0.200	1					
-0.879	-0.238	-0.974	0.260	1				
0.029	-0.117	0.024	0.111	-0.017	1			
0.164	0.161	0.144	-0.153	-0.125	-0.975	1		
0.482	0.214	0.462	-0.209	-0.422	-0.854	0.940	1	
0.102	0.937	0.181	-0.967	-0.250	-0.028	0.059	0.112	1
0.803	0.264	0.834	-0.271	-0.813	-0.522	0.659	0.868	0.201
-0.113	-0.876	-0.198	0.926	0.271	-0.005	-0.024	-0.083	-0.986
-0.853	-0.283	-0.947	0.302	0.973	0.206	-0.343	-0.610	-0.269
-0.122	-0.918	-0.162	0.880	0.196	0.268	-0.316	-0.352	-0.736
1								
-0.191	1							
-0.916	0.279	1						
-0.334	0.640	0.279	1					

all the frequencies but those marked by an asterisk) belonging to the first four vibration–rotation transitions. Frequencies of the $3\nu_7^1 \leftarrow 2\nu_7^0$ and $4\nu_7^2 \leftarrow 3\nu_7^1$ transitions were not included in this joint processing, since a set of frequencies for these transitions did not allow one to determine the constants of these levels separately but only in combinations. The calculated frequencies obtained in this processing as well as the differences of the experimental and the calculated line frequencies are listed in Table I. As seen from Table I almost all the treated lines are well described by the adopted model. However, some regular deviations are observed for spectral lines with small J values which belong to the transitions $\nu_7^1 \leftarrow 0$ and $2\nu_7^2 \leftarrow \nu_7^1$. For the lines with small J of the transition $\nu_7^1 \leftarrow 0$ one can observe that the "plus" sign prevails in the differences between the experimental and the calculated frequencies for P and R branches and the "minus" sign for the Q branch. For the transition $2\nu_7^2 \leftarrow \nu_7^1$ the plus sign prevails in the same differences for Q and R branches corresponding to even values of J, and the minus sign for Q and R branches corresponding to odd values of J. One can conclude from the corresponding diagrams of energy levels that the calculation gives an overestimated value of splitting of c and d components for the levels in the state ν_7^1; we cannot derive certain conclusions for the state $2\nu_7^2$ due to the lack of data. Thus, these regular deviations of the calculated and the experimental data are probably due to inadequate processing of the state ν_7^1 for small J.[2]

The obtained rotational and centrifugal constants and the constants of "ℓ"-splitting for the ground and the excited states ν_7^1; $2\nu_7^2$; $3\nu_7^3$; $4\nu_7^4$ as well as the frequencies of purely vibrational transitions $\nu_7^1 \leftarrow 0$; $2\nu_7^2 \leftarrow \nu_7^1$; $3\nu_7^3 \leftarrow 2\nu_7^2$; $4\nu_7^4 \leftarrow 3\nu_7^3$ together with their correlation matrix are given in Table V. The frequencies of purely vibrational transitions are determined as the differences of vibrational energies of the upper and lower states of the transition $E_v^u - E_v^e$, where E_v^u is the vibrational energy of the upper state and E_v^e is the vibrational energy of the lower state.

[2] It should be noted, however, that these regular deviations are of order of experimental errors.

The results of this investigation enable one to determine to a high degree of accuracy a potential function of anomalously low highly anharmonic vibration ν_7 in C_3O_2 near the bottom of a potential well.

ACKNOWLEDGMENTS

The authors thank Dr. V. I. Rochenkov for considerable help in preparing the C_3O_2 samples.

RECEIVED: January 15, 1982

REFERENCES

1. A. V. BURENIN, E. N. KARYAKIN, A. F. KRUPNOV, AND S. M. SHAPIN, *J. Mol. Spectrosc.* **78,** 181–184 (1979).
2. B. A. ANDREEV, A. V. BURENIN, E. N. KARYAKIN, A. F. KRUPNOV, AND S. M. SHAPIN, *J. Mol. Spectrosc.* **62,** 125–148 (1976).
3. A. V. BURENIN, E. N. KARYAKIN, A. F. KRUPNOV, S. M. SHAPIN, AND A. N. VAL'DOV, *J. Mol. Spectrosc.* **85,** 1–7 (1981).
4. G. HERZBERG, "Infrared and Raman Spectra of Polyatomic Molecules," Van Nostrand-Reinhold, New York, 1945.